Effect of Burnup on ACR-700 3-D Reactivity Devices Cross Sections

M. Dahmani*, G. Marleau and É. Varin
Institut de Génie Nucléaire, École Polytechnique de Montréal,
2900 Boulevard Édouard-Montpetit, Montréal,
Québec, H3T 1J4, Canada

Abstract

Full core analysis of typical power reactors being generally performed using few groups diffusion theory, it is necessary to generate beforehand, using a lattice code, the required few group cross sections and diffusion coefficients associated with each region in the core. For CANDU-type reactors including the Advanced CANDU Reactor (ACR), the problem is more complex because these reactors contain vertical reactivity devices that are located between two horizontal fuel bundles. The usual calculation scheme relies in this case on a 2-D fuel cell calculation to generate the few group fuel properties and on a 3-D supercell calculation for the analysis of the reactivity devices present in the core. Because of its complexity, the supercell calculations are generally performed using simplified fuel geometries. In this paper, the different stages involved in the reactor physics simulations for ACR will be explained focusing particularly on a study of the burnup dependence of the incremental cross section associated with zone control units (ZCU). The use of these incremental cross sections for finite core calculations will also be presented.

KEYWORDS: ACR-700, Reactivity device simulations, 3-D transport calculations

1. Introduction

A full core analysis of the advanced CANDU reactor (ACR) is required to determine departure from criticality as well as the power distribution inside the reactor [1, 2]. This analysis is generally based on a two group solution to the neutron diffusion equation where one assumes that the reactor is composed of homogeneous cells. Since the cells are effectively highly heterogeneous, being composed of a CANFLEX fuel cluster located in a light water cooled pressure tube immersed in heavy water, there is a need to generate beforehand, using a lattice code, the required homogeneous few group cross sections and diffusion coefficients associated with each cell in the core. In addition, the ACR is controlled using reactivity devices, the zone control units (ZCU) that can be inserted along the vertical direction between two horizontal fuel bundles. These control devices are generally simulated in reactor calculations codes by superimposing cross sections and diffusion coefficients perturbations on the homogenized cell

*Corresponding author: Fax. 514-340-4192, E-mail: Mohamed.Dahmani@polymtl.ca

properties. [3] In order to evaluate these cross section perturbations a succession of supercell calculation that involves two fuel cells and the reactivity device itself must be performed.

Here we will discuss the models required to generate the incremental cross sections associated with the ZCU that can be inserted in the ACR. To evaluate these cross sections we need a 3-D assembly model that consists of two horizontal fuel channels and a vertical control device region [4,5]. In fact the control device region may be filled with moderator (no device present), or various materials for the case where only the guide tube is present or in the case where the reactivity device is fully inserted. Because of its complexity, the supercell calculation is generally performed using a simplified geometry. For example, the fuel elements located in a given ring can be homogenized with the coolant surrounding them. The homogenized cross sections required for such a model will be generated using 2-D cell calculations for a fine mesh exact description of a fuel cluster. The impact of the homogenization procedure on the incremental cross sections and on the finite core calculation will be evaluated. We will also analyze the case where two fuel channels have different burnups, and study how the reactivity of the ZCU is affected by this change in local fuel properties.

In this paper, we present the different models used in different stages involved in the reactor physics simulations for the ACR (see Section 2.) using the lattice code DRAGON [6] and the reactor code DONJON [7]. We will focus particularly on the studies and analyses related to the 3-D supercell models used to simulate the ZCU. Reactor calculations using these incremental cross sections will also be presented.

2. Supercell simulation methodology in DRAGON

The ACR-700 fuel bundle is a CANFLEX cluster of 43 fuel pins having different sizes at each ring (see Fig. 1). The fuel is composed of uranium oxide with different enrichment where the central pin contains dysprosium. The coolant located inside the pressure tube is light water

Figure 1: ACR-700 fuel cell cluster.

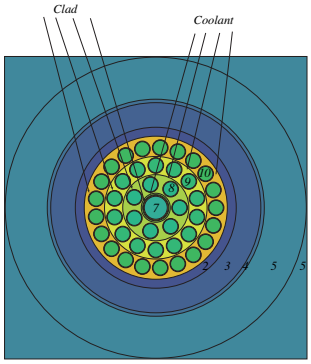

and the moderator located outside the calandria tube is heavy water. The ZCU controller is an off-centered stainless steel plate riding inside a square perforated zirconium guide tube. It is located mid-way between two fuel channels as illustrated in Fig. 2.

2.1 Incremental cross section evaluation

Since the left fuel bundle has a burnup that generally differs from that on the right bundle, the procedure for evaluating the incremental cross sections associated with the ZCU involves

Figure 2: Projections in the $x-y$ (bottom) and $x-z$ (top) planes of the ZCU located between two fuel bundles.

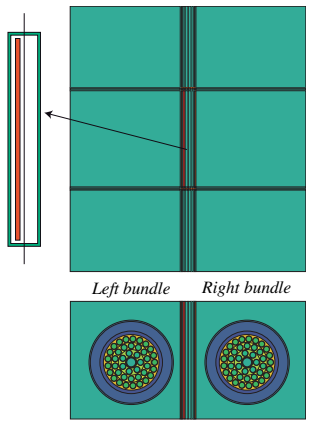

three successive 3-D transport calculations. The first calculation, which is used to evaluated the average supercell few group cross sections in the absence of the reactivity device ($\Sigma^G_{C,x}$) must be performed using a model where the stainless steel plates and the guide tube are replaced with moderator. Assuming that the multigroup cross section $\Sigma^g_{i,x}$ of type x associated with a region of volume V_i sees a flux ϕ^g_i, then $\Sigma^G_{C,x}$ is obtained using:

$$\Sigma^G_{C,x} = \frac{\sum_{g\in G}\sum_i V_i\phi^g_i\Sigma^g_{i,x}}{\sum_{g\in G}\sum_i V_i\phi^g_i} \tag{1}$$

The second step consists in replacing only the ZCU with moderator and repeating the transport calculations to obtain new flux distributions. The resulting homogenized and condensed cross sections $\Sigma^G_{T,x}$, computed using an equation similar to Equation (1) include the effect of the guide tube, weighted by the new flux. Finally, in order to evaluate the incremental cross section associated with the ZCU ($\Delta\Sigma^G_{D,x}$) a third transport calculation must be performed where the guide tube is present and the control plate is fully inserted and occupies a full lattice pitch. The procedure considered to evaluate the incremental cross sections is

$$\Delta\Sigma^G_{D,x} = \Sigma^G_{D,x} - \Sigma^G_{T,x}. \tag{2}$$

The incremental cross sections associated with the guide tube $\Delta\Sigma^G_{T,x}$ can also be obtained by the difference between $\Sigma^G_{T,x}$ and $\Sigma^G_{C,x}$.

2.2 ZCU simulation models

Because of limitations in 3-D geometry, analyzing directly the problem illustrated in Fig. 2 using version 3.04 of the code DRAGON was impossible [8,9]. In addition, even if such a model was available, the fine mesh discretization that would be required to ensure spatial convergence of the flux would be impractical for prospective studies because of the size of the transport problem that would need to be solved. Moreover, taking into account different burnups would imply depleting the fuel in both bundles at different rates. Accordingly, a simplified model where the fine mesh discretization is accounted for by an homogenization process has been selected. Here we will assume that the fuel cluster can be replace by an equivalent four regions annular fuel model.

The main problem we then face consists in selecting the flux distribution that will be used to produce the cross sections associated with the annularized fuel. Because the impact of the ZCU on the flux distribution inside the fuel should be relatively small, we have assumed that a 2-D cell calculation in the exact cluster geometry should provide an adequate flux distribution for the homogenization process. Here, in order to preserve as much information as possible, no energy condensation will be considered and the final 3-D supercell calculations will be performed using the same group structure as that used for the cell calculations. For simplification, we will also assume that the two fuel channels can be burn independently using our 2-D cell model. This assumption, which should be reliable, is similar to that used to produce burnup dependent cell cross sections for the reactor model.

2.3 Homogenization process

Our homogenization model generates 8 different mixtures. Mixture 1 to 4 will represent the pressure tube, gap, calandria tube and the moderator. Mixtures 5 to 8 combine, for each ring of fuel pins, the fuel, the sheathing and an annular region of coolant in contact with the pins. Now two homogenization options could be considered in DRAGON at this point.

The simplest and more standard method is the flux/volume homogenization procedure (see Equation 1). The main advantage of this method is that it will generate cross sections for mixture 1 to 4 that are independent of the coolant and fuel properties. The main drawback is that solving the transport equation on the simplified geometry using these cross sections will result in an eigenvalue and regional reaction rate distributions that differ from the reference solution.

The second alternative is to use the superhomogenization technique [10]. Here, an iterative procedure based on the resolution of the transport equation for the homogenized problem is used to correct the cross sections in such a way that the eigenvalue and regional reaction rate distributions are preserved by the homogenization procedure. The main problem in this case is the fact that the moderator cross sections now depend on the fuel burnup and coolant properties. As a result, the moderator displaced by the ZCU in the left hand cell will differ from that in the right hand cell when the two fuel have different burnups leading possibly to errors in the incremental cross sections associated with the ZCU.

Here we have investigate both homogenization methods and have found (see Section 4.3) that even if they yield relatively large differences in the incremental cross sections the global effect on the final reactor calculation is very small. Accordingly, we will consider only standard flux/volume homogenization procedure for our burnup dependent studies.

3. Model validation

The explicit cell model we have selected is identical to that presented in Fig. 1 except that the fine mesh discretization is not illustrated. Our fine mesh is such that each fuel pin is subdivided into 3 sub regions of equal volume, each of the last three coolant regions is also subdivided into 4 sub regions of equal annular thickness and the moderator region is discretized into 10 annular sub regions. The transport equation is then solved in DRAGON using a collision probability (CP) technique assuming white (isotropic) boundary conditions. The cross section library we selected is an ENDF/B-VI based 89 group WIMS-AECL format library [11].

Note that in the flux calculation module of DRAGON, several leakage options can be used. In fact, one can choose between a k_{eff} eigenvalue problem without leakage and a buckling problem with B_0 and B_1 leakage term [12]. For our supercell calculation, the procedure considered is

Table 1: 3-D supercell k_∞ compared to the 2-D reference calculation

B (GWd/T)	k_∞	Δk_∞ (mk)	
		no SPH	SPH
0.0	1.22237	-9.71	-0.46
0.069	1.18455	-8.97	0.28
0.186	1.17989	-8.88	0.29
3.59	1.13928	-8.23	0.40
31.5	0.82822	-9.00	-0.29

the use of a homogeneous B_1 leakage model with imposed $k_{\mathit{eff}} = 1$, since one expects the supercell to be critical. A similar argumentation is also valid for the supercell involving the ZCU since these are used to maintain the reactor in a critical state. Once the flux distribution at a given burnup has been obtained the homogenization process can then be considered.

3.1 Homogenization effect

Two series of supercell calculations were performed without any device. The first series uses the flux/volume homogenized cross sections and the second the SPH corrected cross sections. The k_∞ values at specific burnup states corresponding to 2-D cell calculation and the Δk_∞ (in mk) representing the difference between the k_∞ generated after the supercell calculation are presented in Table 1. As one can see, the use of the flux/volume weighting method for the cell homogenization can induce differences of up to -9 mk. On the other hand, the values of k_∞ are very close to those of the 2-D cell when using the SPH technique, as expected.

3.2 Tracking effect

In version 3.04 of DRAGON, the equal weights angular quadrature EQ_N [13] is used to select the discrete angles. The number of angles in each octant is then calculated using

$$N_{ang} = \frac{N(N+2)}{2} \tag{3}$$

where N is the order of the quadrature. For the 3-D geometries N can take values between 2 and 16. For all calculations, the track density d_T (tracks/cm^2) also has to be selected. Different tracking options were used to evaluate the ZCU incremental cross sections. A coarse mesh spatial discretization was selected for all these tests. For each case, k_∞ is compared to that obtained using the finer tracking option (16 angles and 400 tracks/cm^2). From Table 2, we can see that when the number of angles and the density of tracks are increased from 2/20 to 4/40, the relative variation of k_∞ change considerably. By continuing to increase the number of angles and the density of tracks, the incremental cross sections get more stable after 8/80. Taking into account the CPU time needed for each calculation, the best selection will correspond to the number of angles 8 and to a density of tracks between 80 and 400.

3.3 Spatial discretization effect

A fine spatial discretization along x, z and y directions is considered here. The discretization along x-axis is not uniform, a coarser mesh being chosen in the fuel cell region while a finer mesh around the devices were selected. As the number of regions increases, the tracking should be finer. For these simulations, 16/400 combination was chosen for the tracking except for the

Table 2: Supercell k_∞ in the presence of the device with various tracking options

EQ_N/d_T	2/20	4/40	8/80	8/200	16/400
k_∞	0.998642	1.002638	1.004007	1.003968	1.003954

Table 3: Supercell k_∞ in the presence of the device with various spatial discretizations

Type of discretization	coarse	x	x-z	x-z-y
Number of regions	96	244	427	854
EQ_N/d_T	2/20	16/400	16/400	16/400
k_∞	0.998642	1.006757	1.007370	1.007379

coarse mesh where 2/20 is used. Here the reference calculation corresponds to the case where a fine discretization is considered along the directions x, z and y, 854 regions are then generated and the CPU time was ≈ 5 days. The results in Table 3 shows that the relative errors when using a coarse mesh model are important. Using a fine mesh along the x axis reduces considerably this relative variation but the CPU time increases considerably (from 20 minutes to more than 3 days). Using a fine mesh along both the x and z increases k_∞ by yet another 0.6 mk but the CPU time increases by one additional day. Finally the use of a fine mesh in all direction does not lead to any substantial improvement in k_∞. Thus, the discretization along the y direction does not affect the results. In conclusion, taking into account the CPU time needed by each model, the best model that will reproduce a relatively accurate values with a relatively small CPU time is the model where a fine discretization along the x direction with a 16/400 tracking.

4. Numerical results

To analyze the effects of fuel burnup on the incremental cross sections associated with ZCU, the 3-D supercell model we propose is composed of two fuel cells with different compositions. In fact, we will represent the global supercell state using B^L and B^R to represent the burnup state in left and right cells. In principle, the supercell properties such as k_∞ and the homogenized cross sections could be affected by these parameters.

4.1 Reference Calculations

The reference calculations were performed assuming both fuel cells at mid-burnup $B^L = B^R = B_r = 9.641 GWd/T$. Moreover, a coarse mesh model is used to minimize the CPU time requirement. The values of the cross sections and the incremental cross sections for ZCU are reported in the Table 4. The properties are homogenized over the complete 3-D supercell and are condensed two energy group with a cut at 0.625 eV. The reactivity $\Delta\rho$ of the device is defined as

$$\Delta\rho(mk) = 1000 \times \left(\frac{1}{k_\infty^T(B^L, B^R)} - \frac{1}{k_\infty^D(B^L, B^R)} \right). \quad (4)$$

4.2 Burnup effect

For these tests, we consider 5 burnup states: fresh fuel condition ($B_1 = 0.0$ GWd/T), nearly fresh fuel containing saturated isotopes (Xe...) ($B_2 = 0.6$ GWd/T) and fuel at exit burnup

Table 4: Reference incremental cross sections for ZCU

	$\Sigma^G_{C,x}$	$\Delta\Sigma^G_{T,x}$	$\Delta\Sigma^G_{D,x}$
Σ^1	3.20E-01	5.88E-05	1.93E-03
Σ^1_a	3.41E-03	1.25E-05	8.89E-05
$\nu\Sigma^1_f$	1.77E-03	-2.21E-06	-7.47E-07
$\Sigma^{1\to1}_{s,0}$	3.09E-01	8.87E-05	1.78E-03
$\Sigma^{1\to2}_{s,0}$	4.43E-01	-4.24E-05	6.18E-05
Σ^2	4.55E-01	-9.81E-04	2.28E-03
Σ^2_a	1.2E-02	6.43E-05	9.00E-04
$\nu\Sigma^2_f$	1.51E-02	3.47E-05	2.45E-04
$\Sigma^{2\to1}_{s,0}$	8.37E-03	1.860E-06	1.42E-05
$\Sigma^{2\to2}_{s,0}$	2.26E-04	-1.04E-03	1.37E-03
$\Delta\rho$ (mk)		-4.32	-50.60

Table 5: Relative variation of the ZCU incremental cross sections for various burnup

	Burnup (GWd/T)				
	0.0	0.6	21.2	25.8	31.5
Σ^1	-1.26	-1.02	1.75	2.52	3.28
Σ^1_a	-5.06	-4.53	5.85	8.24	10.63
$\Sigma^{1\to1}_{s,0}$	-1.09	-0.83	1.15	1.68	2.11
$\Sigma^{1\to2}_{s,0}$	-0.83	-1.58	13.00	18.78	26.45
Σ^2	2.12	1.75	-1.02	-1.22	-0.99
Σ^2_a	-3.15	-2.34	-0.18	-0.35	-0.77
$\Sigma^{2\to1}_{s,0}$	-2.79	-1.47	-3.36	-5.20	-7.34
$\Sigma^{2\to2}_{s,0}$	5.62	4.46	-1.54	-1.75	-1.07
$\Delta\rho$ (mk)	-45.0	-46.0	-61.4	-66.4	-72.7

($B_3 = 21.2$ GWd/T). Two burnups higher than the exit burnup (25.8 and 31.5 GWd/T) have also been considered. Cell properties corresponding to these irradiation levels are actually used in core calculation in standard time-average model. To evaluate the burnup effect on the incremental cross sections, the relative variation δ_B is defined

$$\delta_B = 100 \times \left(\Delta\Sigma^G_{D,x}(B^L, B^R) - \Delta\Sigma^G_{D,x}(B_r, B_r)\right) / \Delta\Sigma^G_{D,x}(B_r, B_r); \tag{5}$$

and the variation of k_∞

$$\delta_B k_\infty = \Delta k_\infty(B^L, B^R) - \Delta k_\infty(B_r, B_r); \tag{6}$$

where

$$\Delta k_\infty(B^L, B^R) = 1000 \times \left[k^D_\infty(B^L, B^R) - k^T_\infty(B^L, B^R)\right]. \tag{7}$$

4.2.1 Effect of uniform burnup

To evaluate the global effect of the burnup on the incremental cross section, the two fuel cells in the supercell will have identical burnup values. Table 5 shows the results for different burnup values.

Table 6: Relative variation of the ZCU incremental cross sections for differential burnup

δ_B	(B_3, B_1)	(B_1, B_r)	(B_1, B_3)	(B_r, B_3)	(B_2, B_3)	(B_2, B_r)	(B_3, B_2)
Σ^1	-1.38	0.04	1.47	1.64	1.46	-0.01	-1.02
Σ^1_a	-3.10	-1.60	1.34	3.83	1.60	-1.45	-2.43
$\Sigma^{1\to1}_{s,0}$	-1.39	0.11	1.33	1.37	1.32	0.09	-1.06
$\Sigma^{1\to2}_{s,0}$	1.36	0.33	5.84	6.15	5.26	-0.57	2.18
Σ^2	-0.59	1.41	1.36	-0.20	1.06	1.12	-0.81
Σ^2_a	-1.93	-1.09	-1.32	-0.15	-1.11	-0.89	-1.15
$\Sigma^{2\to1}_{s,0}$	-2.34	-0.99	-2.78	-1.91	-2.33	-0.50	-1.47
$\Sigma^{2\to2}_{s,0}$	0.30	3.07	3.16	-0.21	2.52	2.45	-0.58
$\delta_B k_\infty(mk)$	-1.0	-5.0	-3.4	1.5	-1.4	-3.0	0.4

For low burnup conditions (0 and 0.6 GWd/T), the relative variations in all the cross sections are relatively small reaching a maximum of 5.62%. At exit burnup (21.2 GWd/T), the variations generally stay at the same level (except for $\Sigma^{1\to2}_{s,0}$) for but change sign. The maximum difference is observed for the slowing down and the fast absorption. These effects can be explained by the fact that as the burnup increases, more and more fission products are formed. This increases the chances of the neutrons to be slowed down or absorbed when interacting with those nuclides. At very high burnups (25.8 and 31.5 GWd/T), the relative variations in the fast absorption and slowing down reach 10 % and 26 % respectively while for the thermal group the variations still remain small ($<$ 8 %). Finally, we observe that the reactivity worth of the ZCU increases (in absolute value) with burnup. This is mainly due to a general increase of the absorption cross section (fast + thermal) with burnup.

4.2.2 Effect of differential burnup

The results we obtained for the case where the two cells have a different burnup are presented in Table 6. In the thermal group, the relative variations in the cross sections remain small. In the fast group, the main variations are observed when the right hand side cell is at the exit burnup (B_3), but again the variations remain lower than 7 %. Note that $\delta_B k_\infty(B_i, B_j) \neq \delta_B k_\infty(B_j, B_i)$ because the ZCU is not centered. The values of $\delta_B k_\infty$ are small so that we expect that using mid-burnup incremental cross sections for reactor calculation should be adequate. Note that a certain linearity is observed concerning the $\delta_B k_\infty$, where

$$\delta_B k_\infty(B_i, B_j) \approx \delta_B k_\infty(B_i, B_r) + \delta_B k_\infty(B_r, B_j) \tag{8}$$

For example we have $\delta_B k_\infty(B_2, B_3) = -1.4 \approx \delta_B k_\infty(B_2, B_r) + \delta_B k_\infty(B_r, B_3) = -1.5$.

4.3 Reactor calculations

To evaluate the burnup effect of incremental cross section on a full core calculation, a ACR-700 core model has been defined in DONJON. This reactor is composed of 300 fuel channels located inside a calandria of 520 cm diameter. To correctly represent this geometry, efforts have been made to obtain a very fine core discretization of $56 \times 60 \times 20$ meshes, respectively in the x, y and z directions [14]. A precise description of the cylindrical outer boundary is carried out, and void boundary conditions are used.

The 2-group properties for the fuel and reflector regions are recovered from DRAGON burnup calculations on the original 2D cell model (See Fig. 1). An age model based on an exit burnup

distribution provided by AECL has been defined and applied to the fuel properties [15]. A mesh-centered finite difference method is used to discretize the multigroup diffusion equation.

Here we have computed the reactivity worth $\Delta\rho$ of the ZCU for the different configurations of fuel burnup in the supercell presented in the previous sections. In each case, two eigenvalue are obtained from DONJON full core calculations, one k_{eff}^{in} for the ZCU fully inserted and one k_{eff}^{out} for the ZCU fully withdrawn. Then $\Delta\rho$ is computed using

$$\Delta\rho = \frac{1}{k_{eff}^{out}} - \frac{1}{k_{eff}^{in}} \tag{9}$$

Using the incremental cross sections generated by a volume-weighted homogenization and an homogeneous fuel burnup B_r, one obtains a ZCU reactivity of -12.6 mk. For the case where the cross sections of the ZCU are computed using a SPH homogenized library, an increase of 0.1 mk in $\Delta\rho$ is observed. This difference is very small indicating that the use of the standard homogenization technique is adequate for our studies. Using in our reactor calculations ZCU incremental cross sections associated with low burnup fuel, results in a maximum variation of 0.1 mk in $\Delta\rho$. On the other hand, for ZCU incremental cross sections associated with high burnup fuel, the reactivity worth becomes more negative with increasing burnup, reaching a minimum of -13.1 mk at $B = 31.5$ GWd/t.

These burnup effects on the ZCU reactivity in the reactor are consistent with the previous results. Effectively, in DRAGON, the ZCU reactivity also becomes more negative as the fuel burnup increases (See Table 5). Here the amplitude of the variations is more limited because the devices occupy their exact place in the reactor and not a periodic position in an infinite reactor.

5. Conclusion

ACR-700 calculation scheme including the 2-D cell, 3-D supercell and 3-D reactor core calculations have been introduced. This includes the 2-D cell, 3-D supercell and 3-D reactor core calculations. Using SPH homogenization technique reduces considerably the differences in k_∞ for the reference supercell with the reactivity device absent. However its impact on reactor core results is very limited. The effect of the depletion on the incremental cross sections associated with ZCU is relatively important when using a uniform burnup. The relative variations of the incremental cross sections, as burnup progresses, increases and becomes important for high burnups especially in fast group. When using a differential burnups, the effects are small. The fact that the device is not very black, off-centered and because of the tight coupling between the cells change considerably the flux spectrum. In core calculations, the use of the incremental cross section at mid-burnup allows an adequate estimation of the reactivity worth of the ZCU.

Acknowledgments

This work was supported in part by the Natural Science and Engineering Research Council of Canada and by Atomic Energy of Canada Limited, and by the Hydro-Québec Chair in Nuclear Engineering.

References

1) J.M. Hopwood, P.S.W. Chan and P.G. Boczar, “The advanced CANDU reactor: Innovations in reactor physics for next CANDU generation” Proceedings of the 13th Pacific Basin Nuclear Conference, Shenzhen, Guangdong, China, October 21-25 (2002).

2) M. Ovanes, P.S.W. Chan and J. Mao, "Reactor physics innovations in ACR-700 design for next CANDU generation", 23rd CNS Annual Conference, Toronto, Canada (2002).

3) E. Varin, R. Roy, R. Baril and G. Hotte, " CANDU-6 operation post-simulation using the reactor physics codes DRAGON/DONJON", Ann. Nucl. Energy, **31**, 2139-2155 (2004).

4) R. Roy, G. Marleau, J. Tajmouati, and D. Rozon, "Modeling of CANDU reactivity control devices with the lattice code DRAGON", Ann. Nucl. Energy, **21**, 115-132 (1994).

5) G. Marleau, R. Roy and B. Arsenault, "Simulation of reactivity control devices in a CANDU-6 reactor using DRAGON", CNS Nuclear Simulation Symposium, Pembroke, Canada (1994).

6) G. Marleau, A. Hébert, and R. Roy, "New computational methods used in the lattice code DRAGON", Topical Meeting on Advances in Reactor Physics, 177, Charleston, SC (1992).

7) E. Varin, A. Hébert, R. Roy and J. Koclas, "A user's guide for DONJON", Technical Report IGE-208 Rev. 2, École Polytechnique de Montréal (2004).

8) G. Marleau, A. Hébert, and R. Roy, "A user guide for DRAGON 3.04", Technical Report IGE-174 Rev. 5, École Polytechnique de Montréal (2000).

9) G. Marleau, "DRAGON theory manual part 1: Collision probability calculations", Technical Report IGE-236 Rev. 1, École Polytechnique de Montréal (2001).

10) A. Hébert, "A consistent technique for pin-by-pin homogenization of a pressurized water reactor assembly", Nucl. Sci. Eng. **113**, 227 (1991).

11) J.D. Irish and S.R. Douglas, "Validation of WIMS-IST", Proc. of 23rd Annual Conference of Canadian Nuclear Society, Toronto, Canada (2002).

12) I. Petrovic and P. Benoist, " BN Theory: Advances and New Models for Neutron Leakage Calculation", Advances in Nuclear Science and Technology, Volume **24** (1996).

13) B. Carlson, "Table of Equal Weight Quadrature EQ_N Over the Unit Sphere", Technical Report LA-4734, Los Alamos National Laboratory (1971).

14) P. Guillemin, " Modélisation du coeur de l'ACR-700'", Report IGE-277, École Polytechnique de Montréal (2005).

15) D. Rozon and S. Wei, " A Parametric study of the DUPIC Fuel Cycle to Reflect Pressurized Water Reactor Fuel Management Study'", Nucl.Sci.Eng. **138**,1-25, 2001.